Light charged particle emission in the matched reactions 280 MeV ^{40}Ar+^{27}Al and 670 MeV ^{55}Mn+^{12}C: Inclusive studies

Craig M. Brown,[1,*] Zoran Milosevich,[1] Morton Kaplan,[1] Emanuele Vardaci,[1,†] Paul DeYoung,[2] James P. Whitfield,[1] Donald Peterson,[2] Christopher Dykstra,[2] Paul J. Karol,[1] and Margaret A. McMahan[3]

[1]*Department of Chemistry, Carnegie Mellon University, Pittsburgh, Pennsylvania 15213*

[2]*Department of Physics, Hope College, Holland, Michigan 49423*

[3]*Lawrence Berkeley National Laboratory, Berkeley, California 94720*

(Received 21 June 1999; published 15 November 1999)

In order to test the statistical model's ability to predict the behavior of relatively light mass systems ($A \approx 67$) with large angular momenta, two matched heavy ion nuclear reactions were used to produce ^{67}Ga* composite nuclei at an excitation energy of 127 MeV. Light charged particles (protons, deuterons, tritons, and α particles) were used as probes to characterize the composite systems and track the deexcitation processes. From these measurements, energy spectra, cross sections, angular distributions, anisotropy ratios, and particle multiplicities were deduced. Measuring many degrees of freedom provides a stringent test for the statistical models. What is found is that models which did well in predicting the behavior of heavy composite systems ($A \approx 150$), are unable to simultaneously reproduce energy spectra, angular distributions, and particle multiplicities for the lighter systems ($A \approx 67$), where angular momentum plays a dominant role. This implies that more rigorous models and/or additional physics are needed to understand the behavior of the hot, high-spin nuclear matter in this mass region. [S0556-2813(99)03712-7]

PACS number(s): 25.70.Gh, 24.60.Dr, 25.75.Gz

I. INTRODUCTION

The behavior of highly excited nuclei has been of considerable and continuing interest in recent years [1,2]. In particular, heavy-ion-induced reactions have often been used to study the evolution of nuclear properties with increasing excitation energy and angular momentum. To track the nuclear deexcitation processes, charged particle emission has been shown to be an effective probe [1], primarily because of its sensitivity to angular momentum and emission barrier effects on the observed light-particle energy spectra, multiplicities, and angular correlations. In the present work we have carried out such measurements and compared the experimental data with theoretical expectations. We were especially interested in studying relatively light-mass systems, where angular momentum might be expected to play a dominant role (due to the relatively small moment-of-inertia), and where few comparisons have been made with theoretical calculations.

The semiclassical statistical model has found wide application in describing the characteristics of compound nuclear emission. Statistical model simulation codes such as CASCADE [3], GANES [4,5], LILITA_N95 [6,7], and MODGAN [8] are powerful tools capable of modeling particle emission, building energy spectra, and angular distributions, and keeping track of quantities such as multiplicities, average emission chain lengths, average nuclear temperatures, and angular anisotropies.

The present study focuses on equilibrated particle emission leading to evaporation residues, with comparisons to calculations performed by the codes LILITA_N95 and MODGAN. In this paper we shall describe the experimental details and report the results derived from inclusive measurements. A succeeding paper will present the particle-particle coincidence data, and discuss the exclusive results.

II. EXPERIMENTAL

To test the statistical model's ability to predict the behavior of relatively light mass systems ($A \approx 67$), where particle emission is dominated by rotational effects (rather than Coulomb effects) [5,9], we have selected for study the two reactions 280 MeV ^{40}Ar+^{27}Al and 670 MeV ^{55}Mn+^{12}C. These reactions are matched to yield the same composite nucleus at the same excitation energy ($E_{\mathrm{c.m.}}+Q$) of 127 MeV. By carrying out the reactions in reversed kinematics [10], particle evaporation spectra of especially good quality may be obtained in detectors placed in the forward hemisphere.

The beams were provided by the 88 Inch Cyclotron facility at the Lawrence Berkeley National Laboratory. The 280 MeV ^{40}Ar beam was collimated to produce a well defined beam spot, 9.8 mm in diameter, on the ^{27}Al target foil of thickness 2.116 mg/cm^2. Similarly, the 670 MeV ^{55}Mn beam for the ^{55}Mn+^{12}C reaction was collimated to produce a beam spot of approximately 8.4 mm in diameter on a C target foil of thickness 2.288 mg/cm^2.

The chamber configurations for the 280 MeV ^{40}Ar +^{27}Al and 670 MeV ^{55}Mn+^{12}C reactions were very similar. Figure 1 shows the chamber setup for the ^{40}Ar+^{27}Al experiment. In both cases, a series of solid state silicon telescopes (SST's) were placed at various angles about the beam, and a CsI(Tl) array was centered 20° above the beam

*Present address: Lawrence Livermore National Laboratory, P.O. Box 808, L-414, Livermore, CA 94551.

†Present address: Dipartimento di Scienze Fisiche, Universita' di Napoli Federico II, I-80126 Naples, Italy.

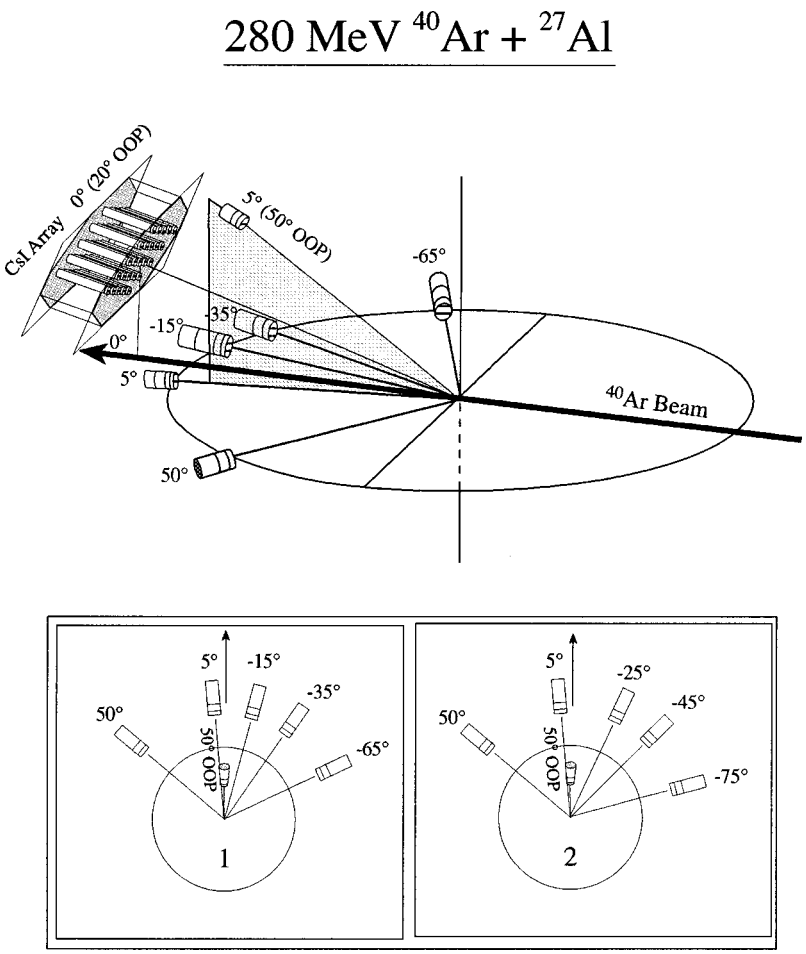

FIG. 1. Chamber configuration for the 280 MeV ^{40}Ar+^{27}Al experiment. The top drawing is a sketch of the detector geometry in the reaction chamber. The bottom panels are representations of two different detector configurations.

line. The purpose of the silicon detectors was to measure energy spectra and angular distributions of the light charged particles, in order to characterize the emitters with respect to spin distributions, temperatures, and reaction mechanisms. The CsI(Tl) array was designed to study small angle particle-particle (p-p) correlations, in order to probe the average particle emission lifetimes and their dependence on emitter spin. These p-p correlation studies will be reported separately in a subsequent publication.

The six silicon telescopes in the 280 MeV ^{40}Ar+^{27}Al experiment were mounted on two rotatable platforms. Three of the telescopes were placed on one platform at 5°,5°(50° out-of-plane, denoted OOP), and 50°, respectively, and were kept stationary throughout the experiment. The three remaining telescopes were placed on the other platform at $-65°$, $-35°$, and $-15°$, respectively, in the first configuration, and subsequently rotated to $-75°$,$-45°$, and $-25°$, respectively, in the second configuration. Each SST consisted of three silicon detectors with thicknesses of approximately 50, 500, and 5000 μm respectively. Lead cover foils of approximately 10 mg/cm^2 were placed in front of five of the telescopes, to shield against low energy electrons and xrays. A beam stopping lead cover foil of 53 mg/cm^2 was placed in front of the 5° in-plane telescope, to stop any elastically scattered beam. The acceptance of each telescope was defined by thick aluminum collimators, with apertures approximately 1 cm diameter.

The 670 MeV ^{55}Mn+^{12}C experiment utilized seven silicon telescopes which were mounted in a manner similar to that described above. Four telescopes were placed on the stationary platform at 0°(35° out-of-plane), 5°,15°, and 35°. The remaining three telescopes were placed on the mobile platform at $-40°$,$-20°$, and $-10°$ in chamber configuration No. 1; $-35°$,$-15°$, and $-5°$ in configuration No. 2; $-50°$,$-30°$, and $-20°$ in configuration No. 3; and $-45°$, $-25°$, and $-15°$ in configuration No. 4. The two telescopes which were positioned at the smallest angles had a fourth detector element of 5000 μm to help measure the high energy protons. Beam stopping cover foils of 84 mg/cm^2 Pb were placed in front of these detectors, while cover foils of 10 mg/cm^2 Pb were placed in front of the other telescopes. In each of the two experiments, the out-of-plane telescope and one in-plane telescope were configured at lab angles corresponding to approximately 90° in the c.m. system.

Solid angles for each SST were determined with an ^{241}Am source of known disintegration rate. The 5.48 MeV α particles from this source also served as an energy marker for the first element of the SST's. Additional energy markers came from ^{148}Gd (3.18 MeV α), and ^{212}Pb (6.05 MeV and 8.78 MeV α) sources. Elastic scattering of ^{1}H, ^{2}H, ^{3}He, and ^{4}He beams (of known energy) from a Au target provided energy calibrations in the 30–60 MeV range. Normalizations between runs and experiments were carried out using the total beam charge measured by a Faraday cup.

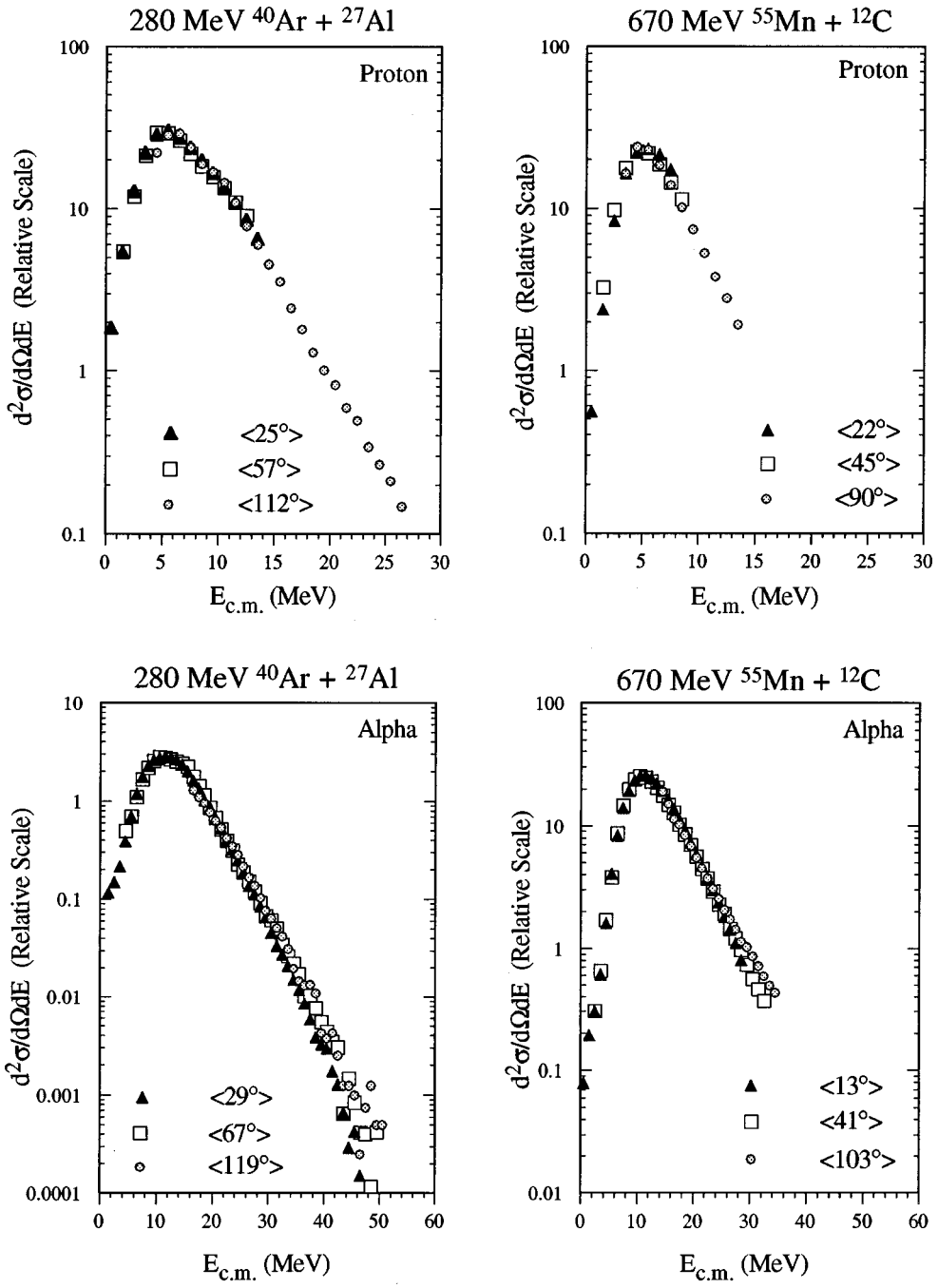

FIG. 2. Inclusive ^{1}H and ^{4}He c.m. energy spectra from the 280 MeV ^{40}Ar+^{27}Al and 670 MeV ^{55}Mn+^{12}C reactions, as labeled. The three superimposed spectra in each panel correspond to different average c.m. angles, as indicated, yet have the same shape.

III. RESULTS

A. Evidence for statistical emission

Figure 2 gives comparisons of the shapes of the ^{1}H/^{4}He center-of-mass (c.m.) energy spectra for the two reactions studied. The 280 MeV ^{40}Ar+^{27}Al data are on the left side of the figure, and the 670 MeV ^{55}Mn+^{12}C data are on the right. The upper two plot frames are for protons and the lower two are for α's. In each plot frame the data consist of a superposition of energy spectra measured at three laboratory angles, corresponding to average c.m. angles as indicated. (Because of the strongly reversed kinematics in these reactions, the laboratory energy spectra often exhibit two kinematic solutions [10]. In transforming spectra to the c.m. system, data from both kinematic solutions were taken into account.)

As Fig. 2 shows, for each case the shapes of the particle energy spectra are essentially independent of c.m. angle, with high-energy slopes corresponding to relatively low effective temperatures. This behavior provides strong evidence for the statistical evaporation from thermally equilibrated compound nuclei. Invariant cross-section maps [11] (not shown here) and c.m. angular distributions (see later) of ^{1}H/^{4}He are also consistent with predominantly evaporative emission. Because of the strongly reversed kinematics

[10] in these reactions, the nonevaporative emissions tend to be focussed backwards in the laboratory, where they are not observed by our detectors.

B. Comparisons of inclusive measurements to LILITA_N95

Simulation codes can be very powerful tools in the analysis of experimental data. They can aid in the identification and deconvolution of multiple emission sources from complex reactions, predict angular distributions, and multiplicities, and test our theoretical models against experimental data. If the physics of the models employed in the calculations is sound, simulation code comparisons to experimental data can be used to extract properties of the reactions which are not directly measurable. Examples of such quantities are the spin distributions, average temperature of the composite system, level density parameters, and emission barrier characteristics.

We shall first present results from calculations with the statistical model code LILITA_N95 [6,7], and compare the model predictions with our experimental data. Then a similar comparison will be carried out using a second statistical model code MODGAN [8], which contains the same physical ingredients (and parameters) as LILITA_N95, but differs in computational methodology. Energy spectra, angular distributions, and particle cross section ratios will be compared between experiment and model calculations, to extract the spin distributions of the 280 MeV ^{40}Ar+^{27}Al and 670 MeV ^{55}Mn+^{12}C reactions, and to test the ability of these codes, and hence their physics content, to predict the evaporative deexcitation behavior of these low mass systems. For the $A=67$ systems as studied here, the rotational energy $E_{\rm rot}$, is a significant fraction of the total excitation energy E^*, a situation which may stretch the applicability of standard statistical models in which the formulation of the Fermi gas level density assumes $E_{\rm rot} \ll E^*$ [12].

It was demonstrated in Fig. 2 above that the ^{1}H/^{4}He center-of-mass energy spectra for both the 280 MeV ^{40}Ar+^{27}Al and 670 MeV ^{55}Mn+^{12}C reactions were superimposable, with the proper normalization factors. This implies that any given center of mass energy spectrum is representative of the others and could, through the appropriate transformation, reproduce any one of the laboratory energy spectra. Therefore, in the comparisons to follow, one representative energy spectrum was chosen to be compared with the LILITA_N95 output.

Figure 3 compares the energy spectra from the 280 MeV ^{40}Ar+^{27}Al reaction to LILITA_N95 simulations. The upper half of the figure is for protons, and the lower half is for α particles. The open circles are the experimental data, and the curves are LILITA_N95 simulations for triangular spin distributions from $J_{\rm min}=0$ to $J_{\rm max}=23\hbar$, $25\hbar$, $27\hbar$, and $54\hbar$. The latter spin was estimated from fusion cross section data [13]. The left frames are laboratory energy spectra at 15°, and the right frames are the corresponding center-of-mass transformations. The proton simulations in Fig. 3 show little spin dependence, as spins $23\hbar$, $25\hbar$, and $27\hbar$ are nearly indistinguishable, and spin $54\hbar$ yields an energy spectrum which is only slightly broader. All of the calculated proton spectra have high energy slopes which are somewhat harder than the data. Since the proton energy spectra are not very sensitive to the initial spin, the spin distribution parameter $J_{\rm max}$ cannot be determined with much certainty from these comparisons.

The α particles in Fig. 3 are much more sensitive to the initial angular momentum in the entrance channel. Here, the calculated curves obtained for $J_{\rm max}=23\hbar$, $25\hbar$, and $27\hbar$ are just distinguishable and the spin $54\hbar$ curve is excessively broad. These fits to the experimental alpha spectra indicate that a spin on the order of $J_{\rm max}=25\hbar$ is associated with the formation of the compound nucleus in the 280 MeV ^{40}Ar+^{27}Al reaction. The curves of spin $23\hbar$ and $27\hbar$ have been chosen to demonstrate the resolution to which this comparative method can select the spin involved. These spins represent the lower and upper bounds of the spin parameter entered into the LILITA_N95 simulation code, and yield a spin parameter ''best'' value of $J_{\rm max}=25\hbar\pm2\hbar$. The spin 54 value is that derived from fusion cross section systematics [13] and is unable to reproduce any of the energy spectra.

Figure 4 compares LILITA_N95 simulations to the 670 MeV ^{55}Mn+^{12}C data. The layout is the same as employed in Fig. 3. The spins chosen for these comparisons are $J_{\rm max}=23\hbar$, $25\hbar$, $27\hbar$, and $37\hbar$, where spins 23, 25, and $27\hbar$ are chosen to fit the spectral data, and spin $37\hbar$ is closer to the value derived from fusion cross section estimates ($42\hbar$) [13].

The proton comparisons in Fig. 4 show the same characteristics as did the proton comparisons of the ^{40}Ar+^{27}Al reaction above. Namely, LILITA_N95 overestimates the slope of the high energy side of the spectrum producing curves which are too broad to fit the data, and showing little sensitivity to spin.

The 670 MeV ^{55}Mn+^{12}C α energy spectra are shown in the lower half of Fig. 4. This provides the best test of the model simulations, as the laboratory energy spectrum exhibits much of the second kinematic solution [10]. The spin parameter required to fit these α spectra can be easily bounded, spin $23\hbar$ falls just below the data points, spin $27\hbar$ grazes the top, and spin $25\hbar$ runs through the data points quite well. A spin of $37\hbar$ is much too large to reproduce the energy spectra. Thus we find that a spin parametrization of $J_{\rm max}=25\hbar\pm2\hbar$ can characterize the 670 MeV ^{55}Mn+^{12}C α energy spectra.

Since the parameter choice of $J_{\rm max}=25\hbar\pm2\hbar$ fits both the 280 MeV ^{40}Ar+^{27}Al and 670 MeV ^{55}Mn+^{12}C reactions, the center-of-mass energy spectra for the two reactions must be very similar. Figure 5 (top) is a superposition of two center-of-mass proton energy spectra, and Fig. 5 (bottom) is a superposition of two center-of-mass α energy spectra. In each case there is an inclusive energy spectrum from the 280 MeV ^{40}Ar+^{27}Al and 670 MeV ^{55}Mn+^{12}C reactions, normalized to their respective peaks. The proton spectra agree rather well up to about 7 MeV, but there are significant deviations in the high energy portions of the spectra, where the ^{55}Mn+^{12}C curve falls off much faster than the ^{40}Ar+^{27}Al spectrum. The α spectra in the lower part of Fig. 5, however, match very well in all energy regions.

Since the proton energy spectra simulated by LILITA_N95 were not very sensitive to the spin input parameter, and since

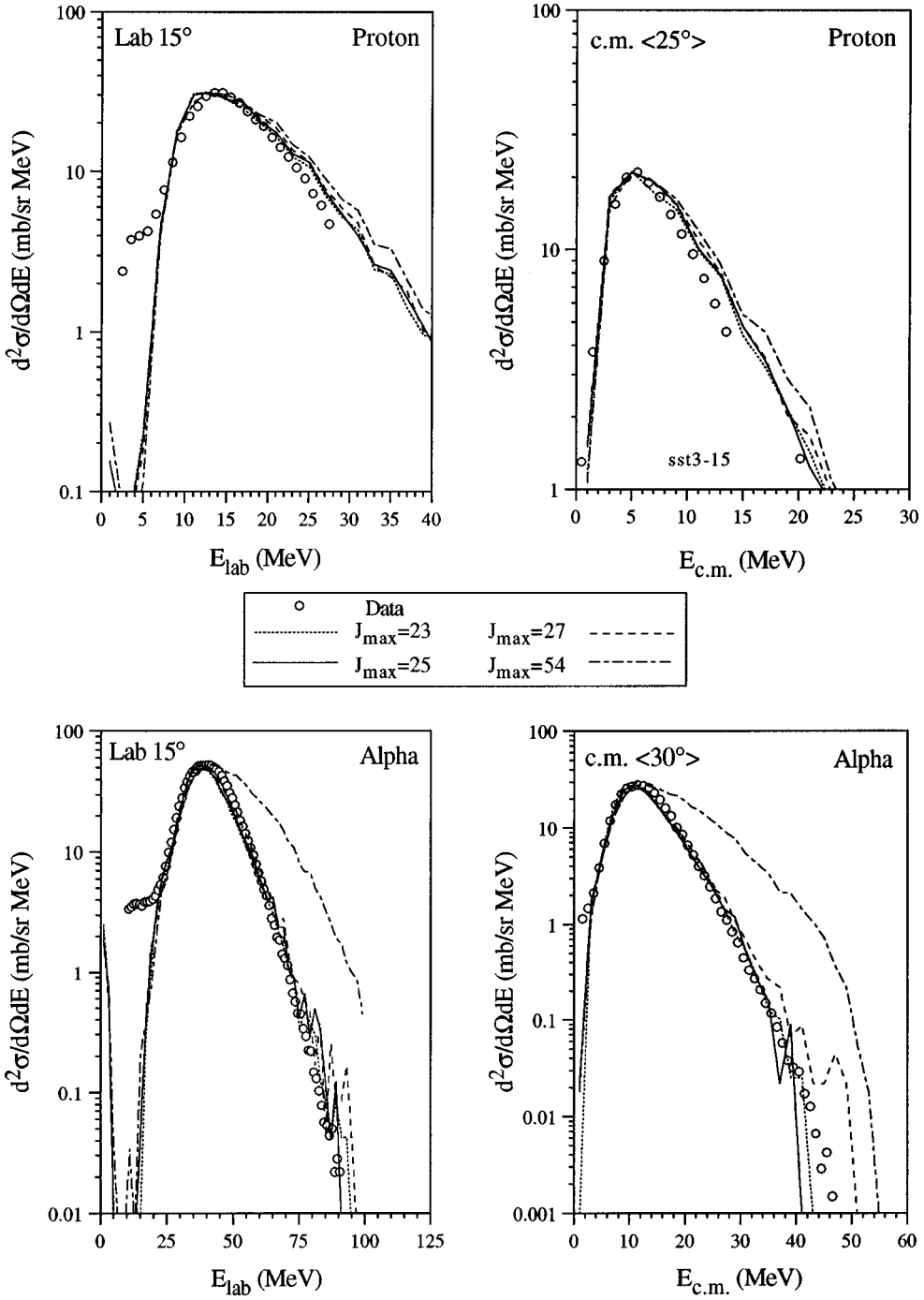

FIG. 3. Inclusive proton (top) and α (bottom) energy spectra for the 280 MeV ^{40}Ar+^{27}Al reaction, compared with LILITA_N95 simulations (curves) for spin parameters of J_{max}=23, 25, 27, and 54$\hbar$. The left (right) panels show laboratory (c.m.) energy spectra for both data and calculations.

the 670 MeV ^{55}Mn+^{12}C and 280 MeV ^{40}Ar+^{27}Al reactions are matched in excitation energy, one might expect better overlap of the proton spectra than shown in Fig. 5 (top). We suspect there might be a calibration problem with the 670 MeV ^{55}Mn+^{12}C proton energy spectra, whose high energy slopes depend strongly on the thick Si stopping detectors at the back of the SST's. For α's measured in these same telescopes, the shorter ranges effectively minimize such effects. Focusing on the α particle spectra in Fig. 5 (bottom), and recalling the sensitivity of LILITA_N95's α spectra to the spin, we find no evidence from the spectra to suggest that there is a significant difference in the spin distributions between the 280 MeV ^{40}Ar+^{27}Al and 670 MeV ^{55}Mn+^{12}C systems. This is surprising, since the two entrance channels were selected specifically to produce different spin distributions.

It is not difficult to demonstrate that the 280 MeV ^{40}Ar +^{27}Al and 670 MeV ^{55}Mn+^{12}C reactions really do yield composite nuclear systems with significantly different spin

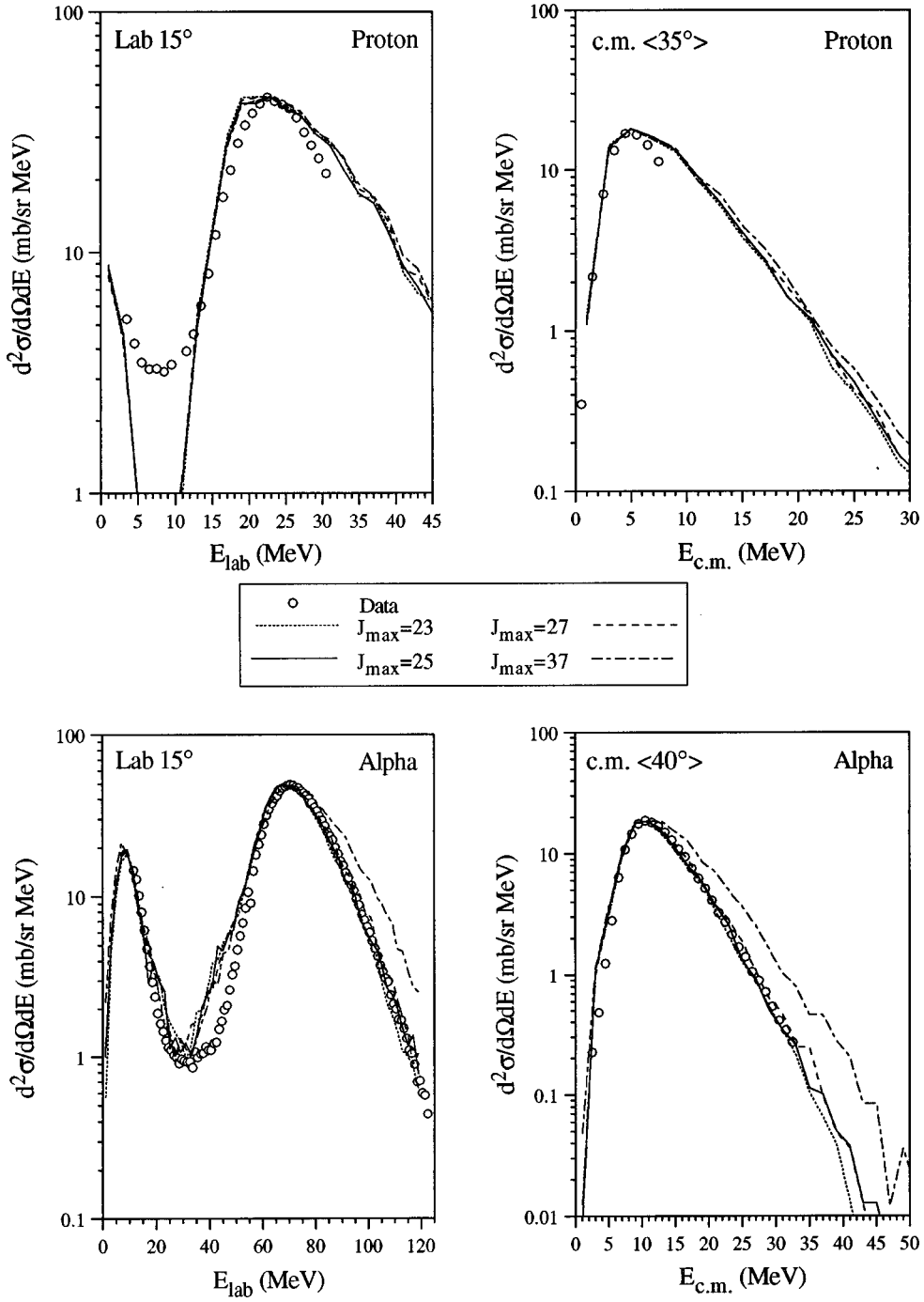

FIG. 4. Inclusive proton (top) and alpha (bottom) energy spectra for the 670 MeV ^{55}Mn+^{12}C reaction, compared with LILITA_N95 simulations (curves) for spin parameters of J_{max}=23, 25, 27, and 37$\hbar$. The left (right) panels show laboratory (c.m.) energy spectra for both data and calculations.

distributions. Figure 6 gives a superposition of the inclusive c.m. α angular distributions for the two reactions, normalized to each other at $\langle\theta_{c.m.}\rangle=0°$. It is clear that the data for the 280 MeV ^{40}Ar+^{27}Al reaction exhibits greater angular anisotropy, as would be expected from a larger value of J_{max} in the entrance channel. We shall return to a more quantitative discussion of the particle angular distributions below.

Given the parameters derived from successfully fitting the α spectra, LILITA_N95 is unable to fit the proton energy spectra nearly as well. The proton energy spectra generated by LILITA_N95 are too broad and are not appreciably narrowed by lowering the spin parameter J_{max}. A more effective way to adjust the high energy slope is through a reduction of the nuclear temperature. This can be accomplished by increasing the level density parameter a, as $T=\sqrt{U/a}$, where T is the nuclear temperature and U is the excitation energy of the daughter nucleus. In the context of the Fermi gas model, the level density parameter can have values ranging from a

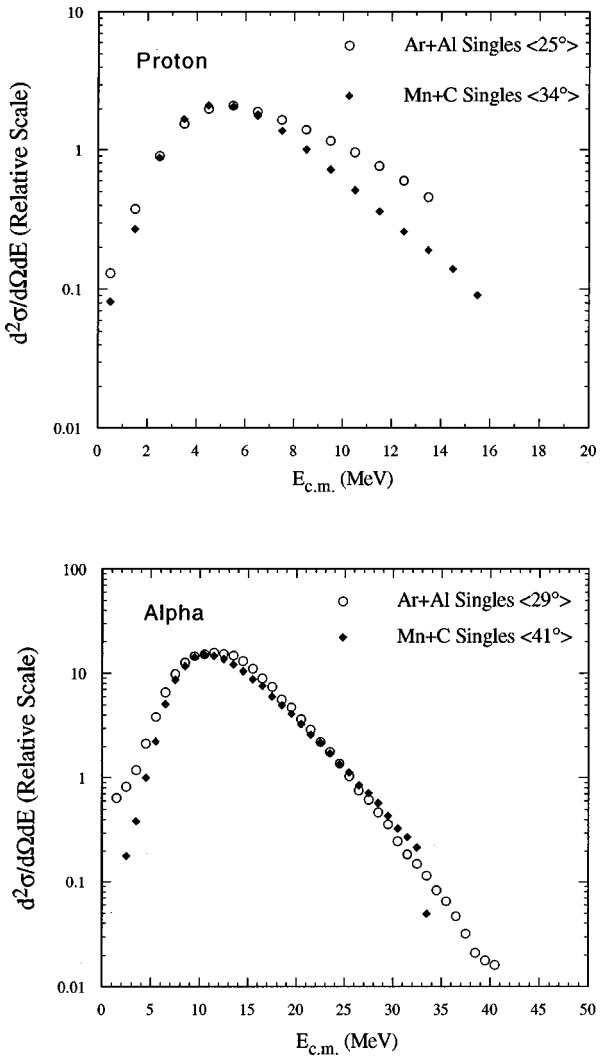

FIG. 5. Comparison of inclusive particle c.m. energy spectra between the 280 MeV ^{40}Ar+^{27}Al and the 670 MeV ^{55}Mn+^{12}C reactions. The top panel compares proton spectra and the bottom panel compares α spectra.

$=A/15$ MeV^{-1} to $a=A/8$ MeV^{-1} [12,14–16]. The simulations in Figs. 4–6 used a level density parameter of $a=A/10$ MeV^{-1}. If this value is changed to $a=A/8$ MeV^{-1}, the energy spectra fall off more rapidly. Figure 7 demonstrates this by comparing the LILITA_N95 spectra at a laboratory angle of 15° with the ^{55}Mn+^{12}C data. The high energy portion of the proton spectrum is matched more closely with this new value of a. The α particle energy spectra are affected in the same way as the proton spectra, and the curve that fit with $a=A/10$ MeV^{-1} now falls below the experimental data, when $a=A/8$ MeV^{-1} is used instead. If this latter value of the level density is more realistic for this system, the calculated α spectra could be adjusted by increasing the spin to approximately $28\hbar$, thereby restoring agreement with the data.

The low energy side of the proton energy spectra are not significantly affected by changing the level density parameter. In this energy region, it is the barrier curvature associated with the transmission coefficients which determines the

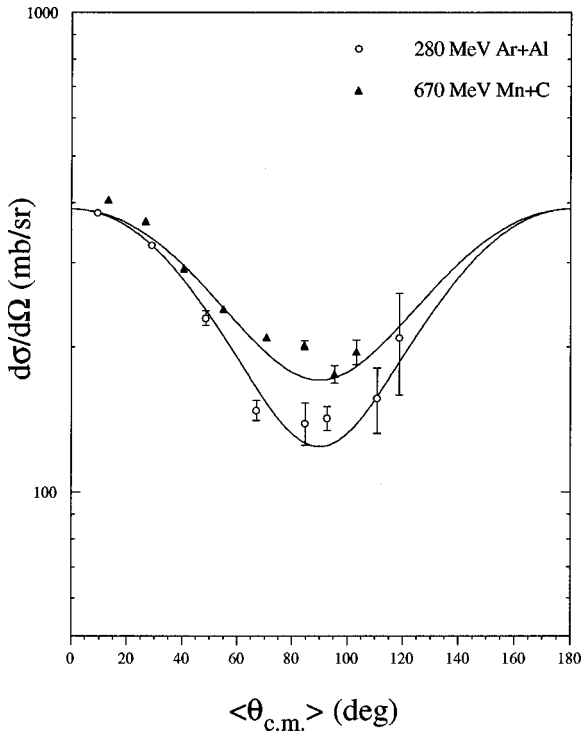

FIG. 6. Inclusive α c.m. angular distributions for the 280 MeV ^{40}Ar+^{27}Al and 670 MeV ^{55}Mn+^{12}C reactions, demonstrating the difference in the spin distributions of the two systems. The ^{55}Mn+^{12}C data have been normalized to the ^{40}Ar+^{27}Al data at 0°.

shape. Figure 8 contains the center of mass proton and α energy spectra overlaid with LILITA_N95 simulations run with barrier curvatures ranging from $\hbar\omega=0$ through 4. In the case of $\hbar\omega=0$, the transmission coefficients reduce to the sharp cutoff approximation where only particles whose energies exceed the Coulomb plus centrifugal barriers are emitted. The proton spectrum is fit very well by values of $\hbar\omega=0$ or 1, and the α spectrum is fit nicely by $\hbar\omega=3$. Although the spectral data in Fig. 8 is from the 670 MeV ^{55}Mn+^{12}C reaction, a review of Fig. 5 implies that the above observations will apply equally well to the 280 MeV ^{40}Ar+^{27}Al reaction.

The angular distributions derived from center-of-mass energy spectra also contain information about the spin of the composite system. As the experimental angular distributions are calculated by integration of the center of mass energy spectra, they are less likely to be strongly affected by uncertainties in the energy calibrations than the high energy slopes of the energy spectra. Figure 9 displays the proton and α c.m. angular distributions from both the 280 MeV ^{40}Ar+^{27}Al and 670 MeV ^{55}Mn+^{12}C experiments. Each plot contains a set of experimental data points with three simulated curves superimposed. The spin values used in these LILITA_N95 simulations are $J_{max}=40\hbar$, $54\hbar$, and $60\hbar$ for the ^{40}Ar+^{27}Al reaction, and $J_{max}=25\hbar$, $37\hbar$, and $40\hbar$ for the ^{55}Mn+^{12}C reaction.

The proton angular distributions are relatively flat indicating that there is little dependence on emitter spin in the simulations. The α angular distributions exhibit much more anisotropy than do the protons, and the sensitivity of the simulation to the spin parameter can be seen. The data are

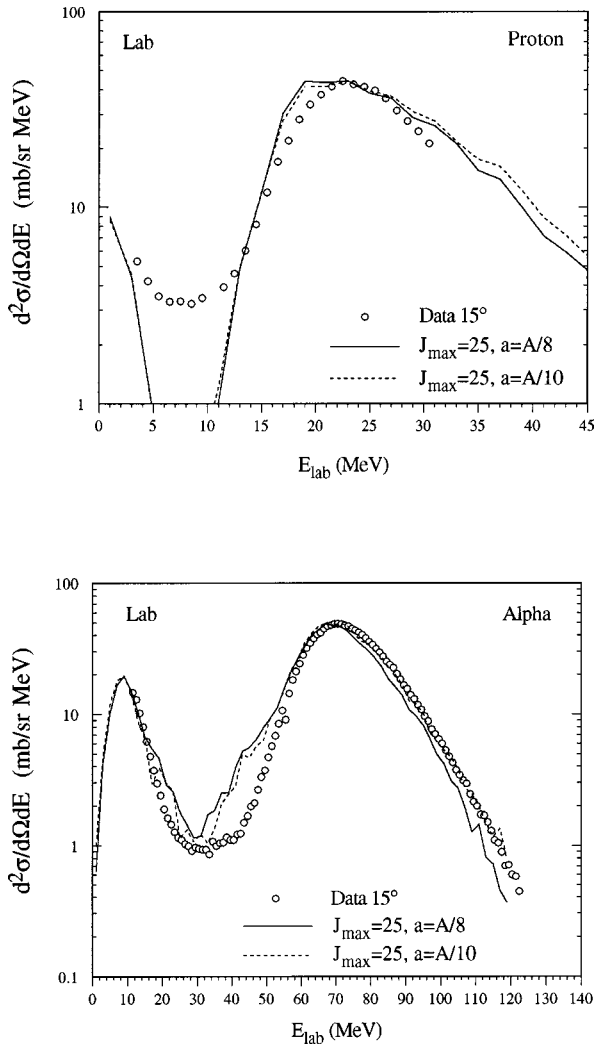

FIG. 7. Inclusive ^{1}H and ^{4}He spectral data (laboratory system) for the 670 MeV ^{55}Mn+^{12}C reaction, compared with LILITA_N95 simulations using $J_{max}=25\hbar$ and level density parameters $a=A/8$ and $a=A/10$, as indicated.

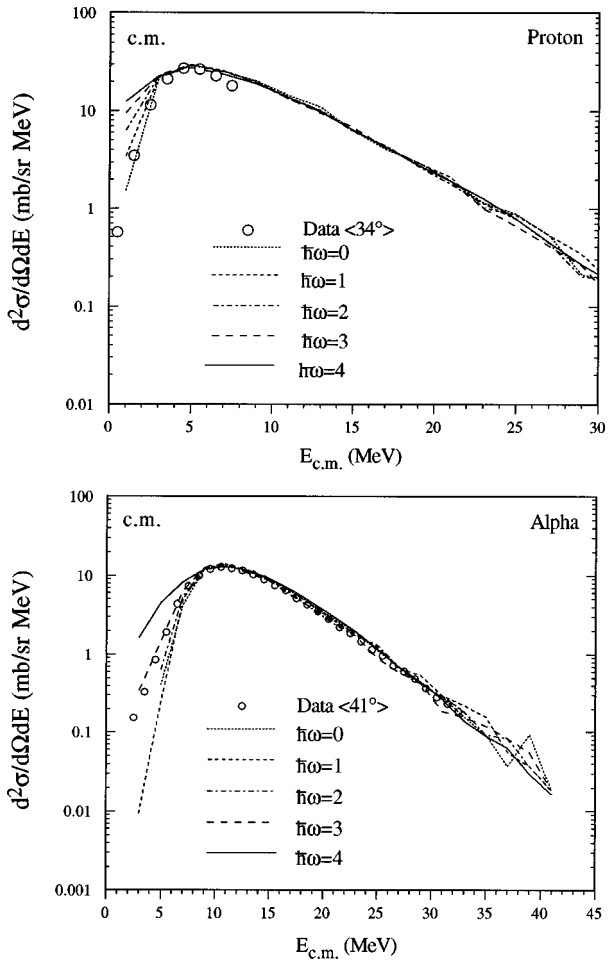

FIG. 8. Inclusive ^{1}H and ^{4}He spectral data (c.m. system) for the 670 MeV ^{55}Mn+^{12}C reaction, compared with LILITA_N95 simulations using $J_{max}=25\hbar$ and barrier curvatures $\hbar\omega=0$, 1, 2, 3, and 4.

consistent with symmetry about 90° in the c.m. The α angular distribution for the ^{40}Ar+^{27}Al reaction can be fit reasonably well with $J_{max}=54\hbar$, although a value of $60\hbar$ does just about as well. This comparison yields a spin parametrization of $54\hbar\pm6\hbar$. The main point is that a spin of the order of $54\hbar$ is required to fit this angular distribution, and a spin of $25\hbar$, which fit the energy spectra, gives far too shallow a curve. The spin $25\hbar$ curve is not plotted in this frame, however, it can be seen in the ^{55}Mn+^{12}C frame to the right along with the spin $40\hbar$ curve. The scales and frame sizes are identical so that a visual manipulation can be made. Thus, the spin $25\hbar$ will appear as much above the spin $40\hbar$ curve in the ^{40}Ar+^{27}Al frame as it does above the spin $40\hbar$ curve in the 670 MeV ^{55}Mn+^{12}C frame.

For the 670 MeV ^{55}Mn+^{12}C reaction, the data are fit very nicely by the spin $37\hbar$ curve. The spin $40\hbar$ curve would also fit reasonably well, and with a slightly higher normalization would pass through the data points. These comparisons yield a spin value of $J_{max}=37\hbar\pm3\hbar$, substantially lower than found for the ^{40}Ar+^{27}Al reaction above, but still significantly higher than derived from fitting the energy spectra.

C. Comparisons of inclusive measurements to MODGAN

In light of discrepancies found in comparisons of several different statistical model codes [17], it is worthwhile to make comparisons with experimental data using more than one statistical model code. Such a procedure may serve to increase one's confidence in the codes as well as confirm consistency in the properties derived from the data using these codes. Since MODGAN [8], by design, contains the same basic physics as LILITA_N95 (i.e., the same formulations of the level-density and the transmission coefficients), it is a good choice for making additional comparisons. Furthermore, MODGAN has several new features, such as deuteron and triton particle evaporation, which have not been extensively tested against experimental data.

Figures 10 and 11 display inclusive proton, deuteron, triton and α energy spectra for the 280 MeV ^{40}Ar+^{27}Al reaction. The open circles are the experimental data, and the curves are MODGAN simulations with spin parameters $J_{max}=25\hbar$, $37\hbar$, and $54\hbar$. In each of the two figures, lab spectra are given on the left and the corresponding c.m. spectra are

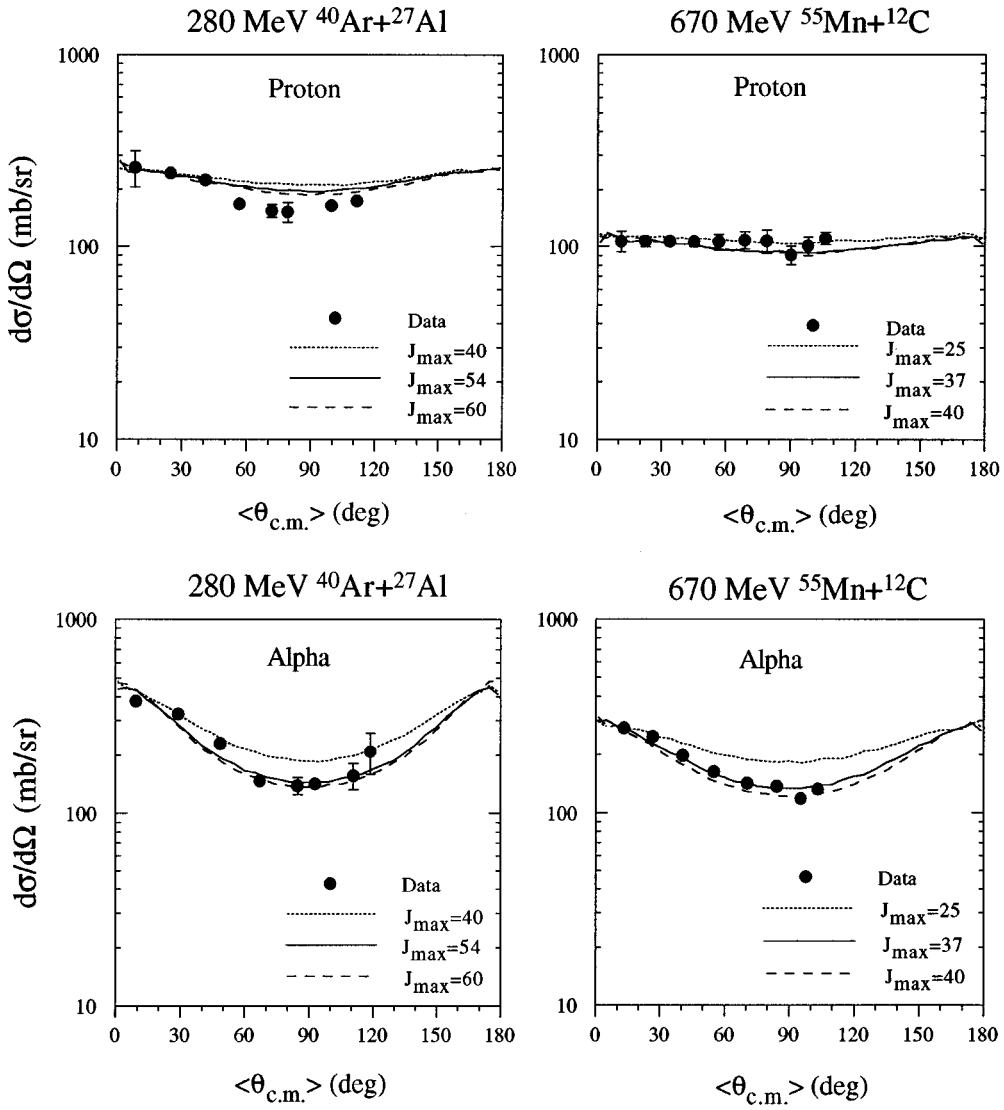

FIG. 9. Comparisons of inclusive ^{1}H and ^{4}He c.m. angular distributions with LILITA_N95 simulations for the 280 MeV ^{40}Ar+^{27}Al and 670 MeV ^{55}Mn+^{12}C reactions. Simulations are shown for several values of the spin parameter J_{max} as indicated.

on the right. The proton energy spectra are reproduced moderately well by all three simulations, reaffirming their insensitivity to angular momentum, and in agreement with the results from LILITA_N95 shown in Fig. 3. The deuteron spectra have more sensitivity to the spin than the protons. The low energy sides of the spectra are overestimated by the calculations, and the high energy sides are best matched with a spin of $54\hbar$. The lower spin values would fit better if a barrier adjustment was made in the model to shift the curves to higher energies [1]. The triton energy spectra behave similarly to the deuteron spectra, with even greater dependence on angular momentum, as can be seen from the spread in the simulation curves. The low energy sides are overestimated by the simulations and a spin of $37\hbar$ most closely reproduces the high energy data. A shift in the effective emission barrier seems to be required here also to fit the data. The low energy sides of the alpha spectra are fitted by MODGAN and the entire spectral shapes are very well reproduced using a spin of $25\hbar$, in agreement with the earlier LILITA_N95 comparison in Fig. 3.

Figures 12 and 13 make the same MODGAN comparisons to the 670 MeV ^{55}Mn+^{12}C energy spectra as Figs. 10 and 11 did for the 280 MeV ^{40}Ar+^{27}Al reaction. Figure 12 shows laboratory and center-of-mass spectra for protons and deuterons. The experimental center-of-mass spectra are actually combinations of data taken from two spectra measured at different laboratory angles, to yield a more complete energy spectrum. In this comparison, the proton spectra simulated by MODGAN are broader than the data. The deuteron laboratory and center-of-mass spectra indicate similar features, however, the high energy slope is better reproduced using a spin of $25\hbar$ in the simulation.

Figure 13 compares the triton and α energy spectra to MODGAN predictions. As with the protons and deuterons, the triton laboratory energy spectrum at 15° was instrumentally truncated and the center-of-mass spectrum was constructed using two additional lab angles normalized to the overlapping points. This triton spectrum, similar to the triton spectrum in the 280 MeV ^{40}Ar+^{27}Al reaction, is fit (without barrier readjustment) using a spin of $37\hbar$ and is overesti-

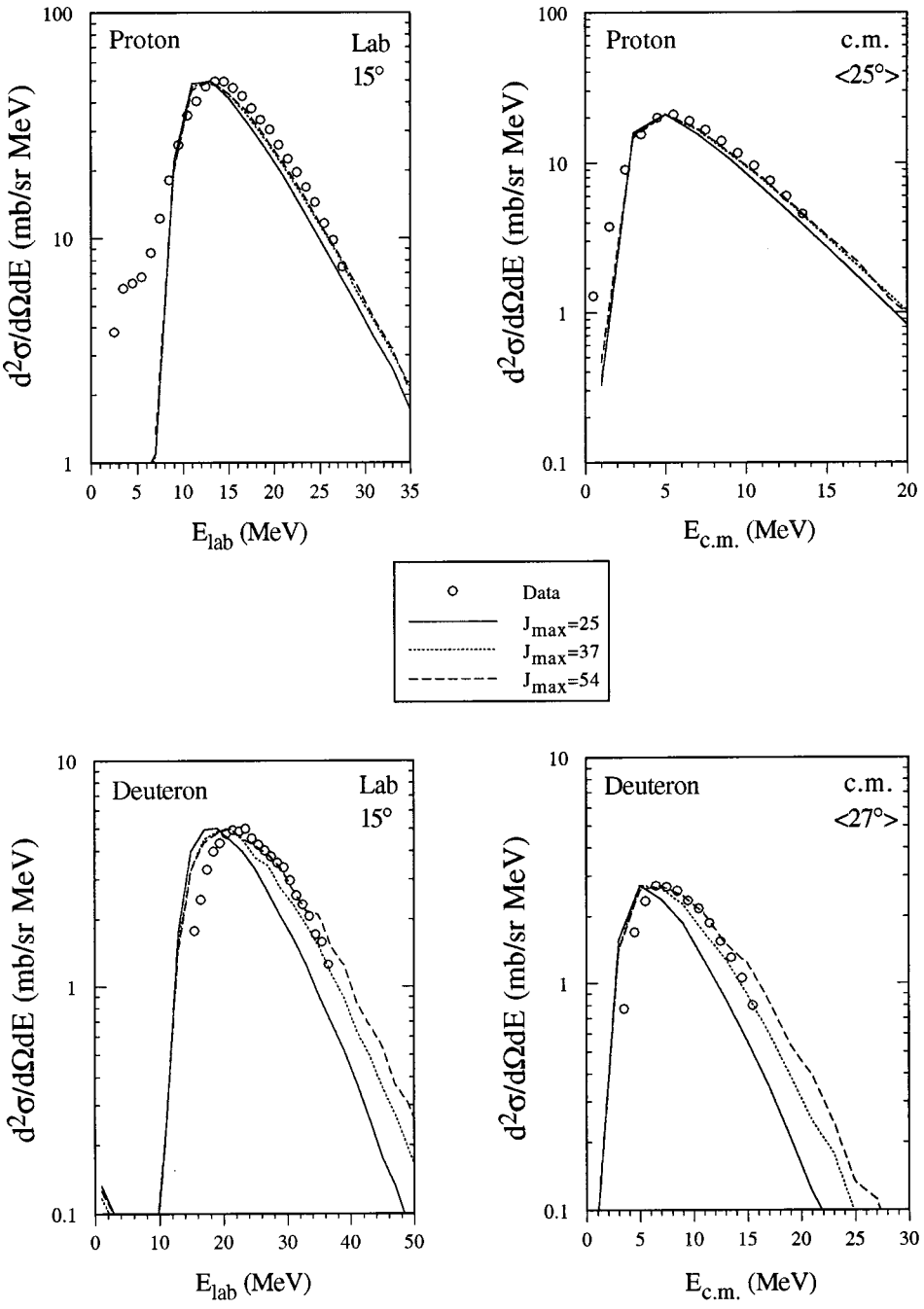

FIG. 10. Inclusive ^{1}H and ^{2}H energy spectra for the 280 MeV ^{40}Ar+^{27}Al reaction, compared with MODGAN simulations using spin parameters J_{max}=25, 37, and 54$\hbar$. Protons are shown in the upper panels and deuterons in the lower panels, with laboratory spectra on the left and c.m. spectra on the right.

mated on the low energy side leading to a shallower trough between the first and second kinematic solutions in the laboratory spectrum. The α spectrum, on the other hand, is reproduced very nicely over the entire energy range with a spin of 25$\hbar$.

Angular distribution comparisons for the 280 MeV ^{40}Ar +^{27}Al reaction are presented in Fig. 14, and those for the 670 MeV ^{55}Mn+^{12}C reaction are displayed in Fig. 15. The open circles are experimental data for the indicated particle (proton, deuteron, triton, and α), and the curves are MODGAN angular distributions obtained using spins of 25, 37, and 54$\hbar$. In each case, the anisotropy of each curve increases with increasing spin. When superimposing the calculations and the data, the simulated curves were normalized to each other at 0°, and adjusted to best fit the data. As can be seen, the spin 54$\hbar$ curve gives the best reproduction of the ^{40}Ar +^{27}Al data, and the spin 37$\hbar$ curve yields good agreement with the ^{55}Mn+^{12}C data points. These spin values (J_{max} =54$\hbar$ and 37$\hbar$) are the same as determined earlier (see Fig. 9) from the LILITA_N95 simulations.

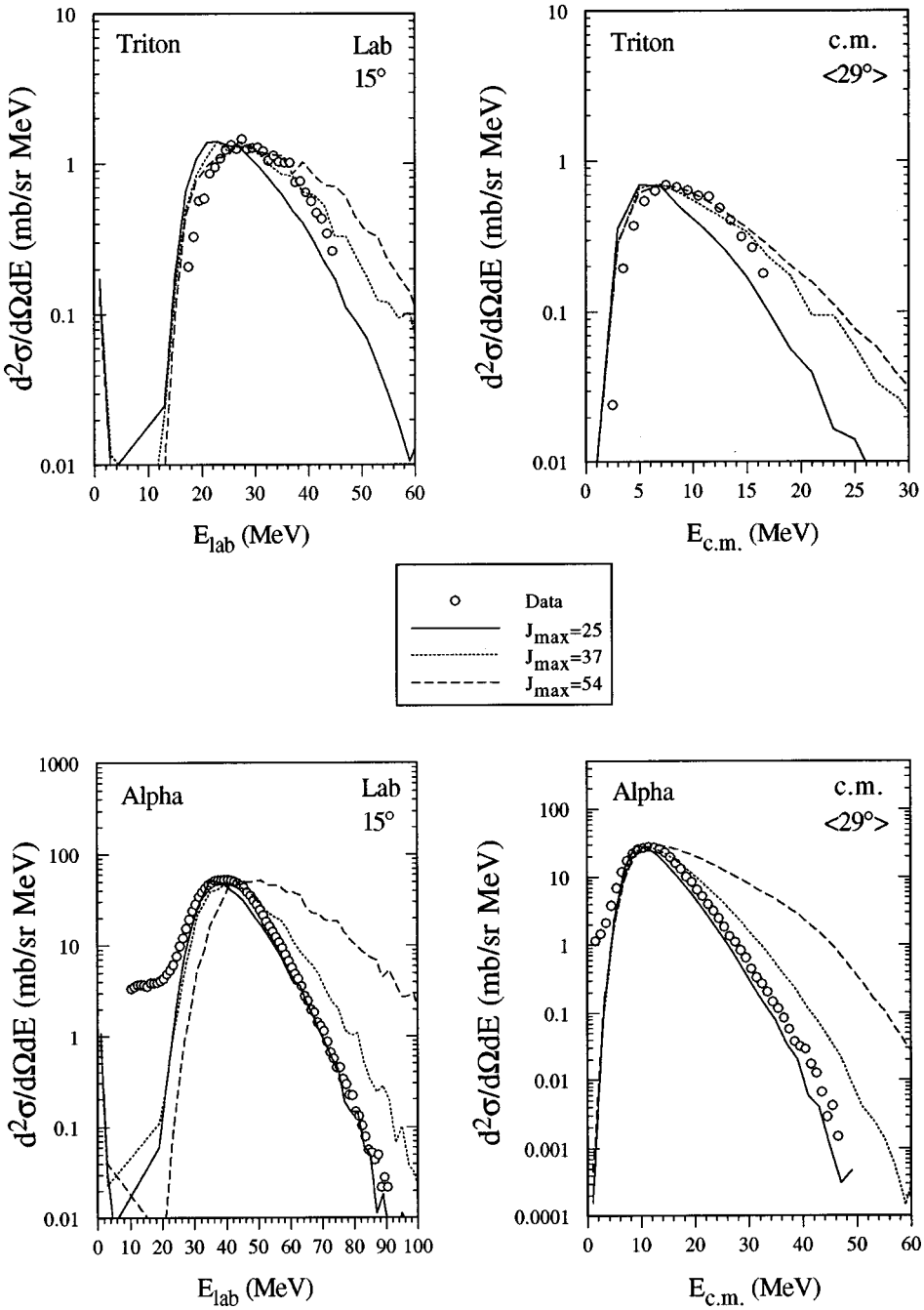

FIG. 11. Inclusive ^{3}H and ^{4}He energy spectra for the 280 MeV ^{40}Ar+^{27}Al reaction, compared with MODGAN simulations using spin parameters J_{max}=25, 37, and 54$\hbar$. Tritons are shown in the upper panels and alphas in the lower panels, with laboratory spectra on the left and c.m. spectra on the right.

In addition to calculations of energy spectra and angular distributions, statistical model simulation codes predict particle multiplicities, which may also be compared with experimental measurements. The LILITA_N95 code is particularly useful in this respect, as it generates detailed event files which may subsequently be sorted using selective criteria, such as the number of occurrences and coincidences of a given particle type or pair. From these quantities, ratios of particle multiplicities can be obtained, eliminating the need for absolute cross sections when making comparisons to experimental data.

The α/proton ratios for the 280 MeV ^{40}Ar+^{27}Al and 670 MeV ^{55}Mn+^{12}C reactions are measured as 1.16 $\pm$0.12 and 0.79 $\pm$ 0.12, respectively. The corresponding ratios calculated by LILITA_N95 and MODGAN are, respectively, 0.45 and 0.36 for spin 25$\hbar$, 0.66 and 0.58 for spin 37$\hbar$, and 1.21 and 1.09 for spin 54$\hbar$. (In the simulations, the multiplicity ratio depends on the entrance channel spin and the composition of the system, but not on the individual identities of the reacting nuclei.) The 280 MeV ^{40}Ar+^{27}Al experimental α/proton ratio is matched by LILITA_N95 simulations using a spin of 54$\hbar$, and the 670 MeV ^{55}Mn+^{12}C experimental results can be matched by LILITA_N95 with a spin of 41$\hbar$. MODGAN gives somewhat lower ratios for the same spin parametrizations, but the differences are fairly small and probably indicative of the reliability of the calculated multiplicity ratios. These values are in very good agreement with the spins derived from

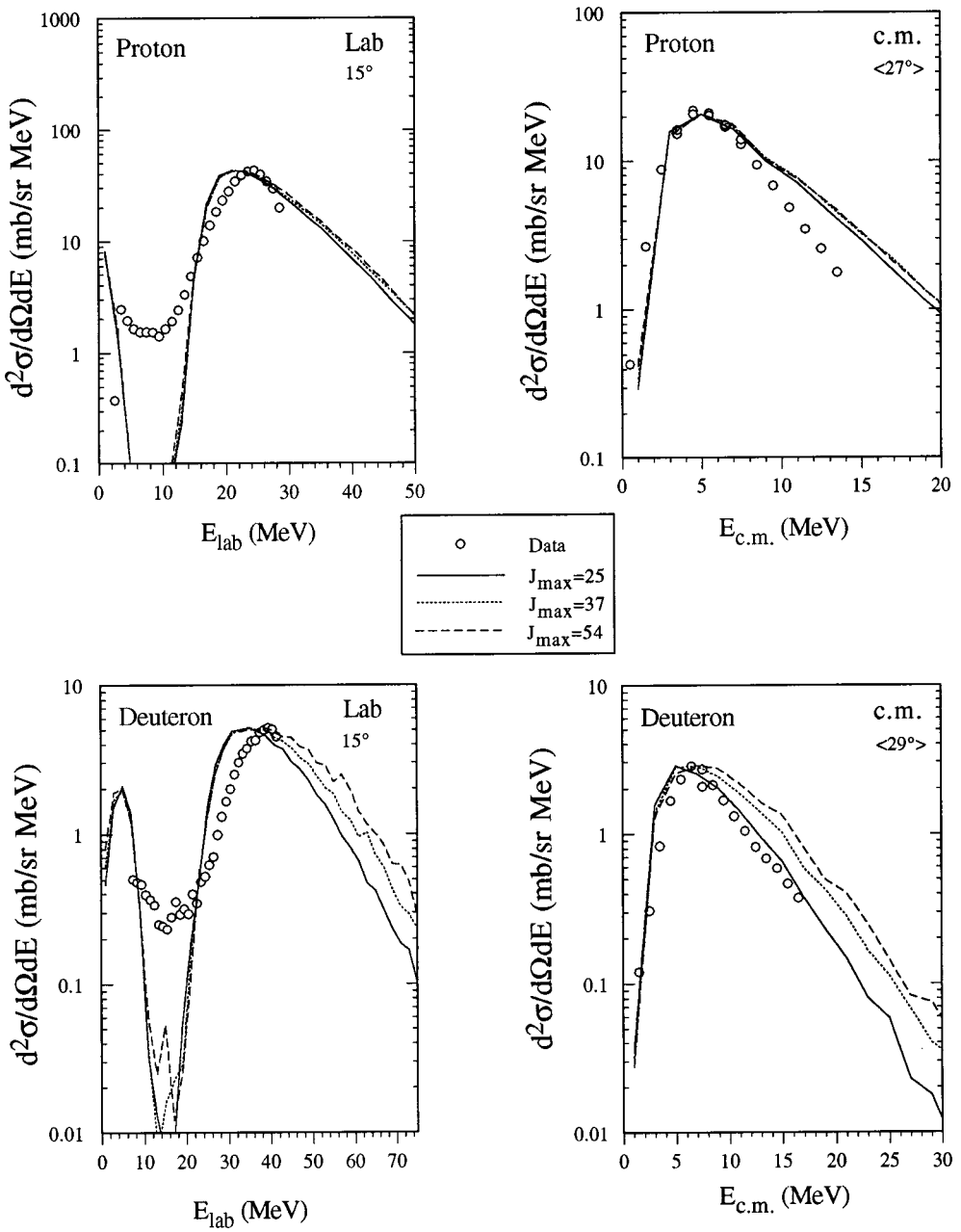

FIG. 12. Inclusive ^{1}H and ^{2}H energy spectra for the 670 MeV ^{55}Mn+^{12}C reaction, compared with MODGAN simulations using spin parameters J_{max}=25, 37, and 54$\hbar$. Protons are shown in the upper panels and deuterons in the lower panels, with laboratory spectra on the left and c.m. spectra on the right.

the angular distribution data for the two reactions, in contrast to the much lower spins suggested by the α energy spectra.

IV. DISCUSSION

Reduced emission barriers [1] play an important role in the fitting of light particle energy spectra with statistical model simulations. Systematic studies [1] indicate that proton evaporation from emitters near atomic number 31 (the present case) exhibit effective barriers substantially lower than corresponding fusion barriers [18], whereas for α emission in this Z region the difference is very small [1]. The two computer codes discussed above, LILITA_N95 and MODGAN, each take account of these effects by means of built-in empirical formulations of the particle emission barriers. Hence the resulting simulations are able to reproduce the peak positions in the experimental spectra rather well.

The effective barrier parametrization that has been applied to the proton emission simulations can also be applied to deuteron and triton emission, scaling by the reduced masses. When this is done, the maxima in the simulated spectra appear at slightly lower energies than the experimental data. The experimental deuteron c.m. energy spectra appear shifted about 1 MeV higher in energy, compared to the

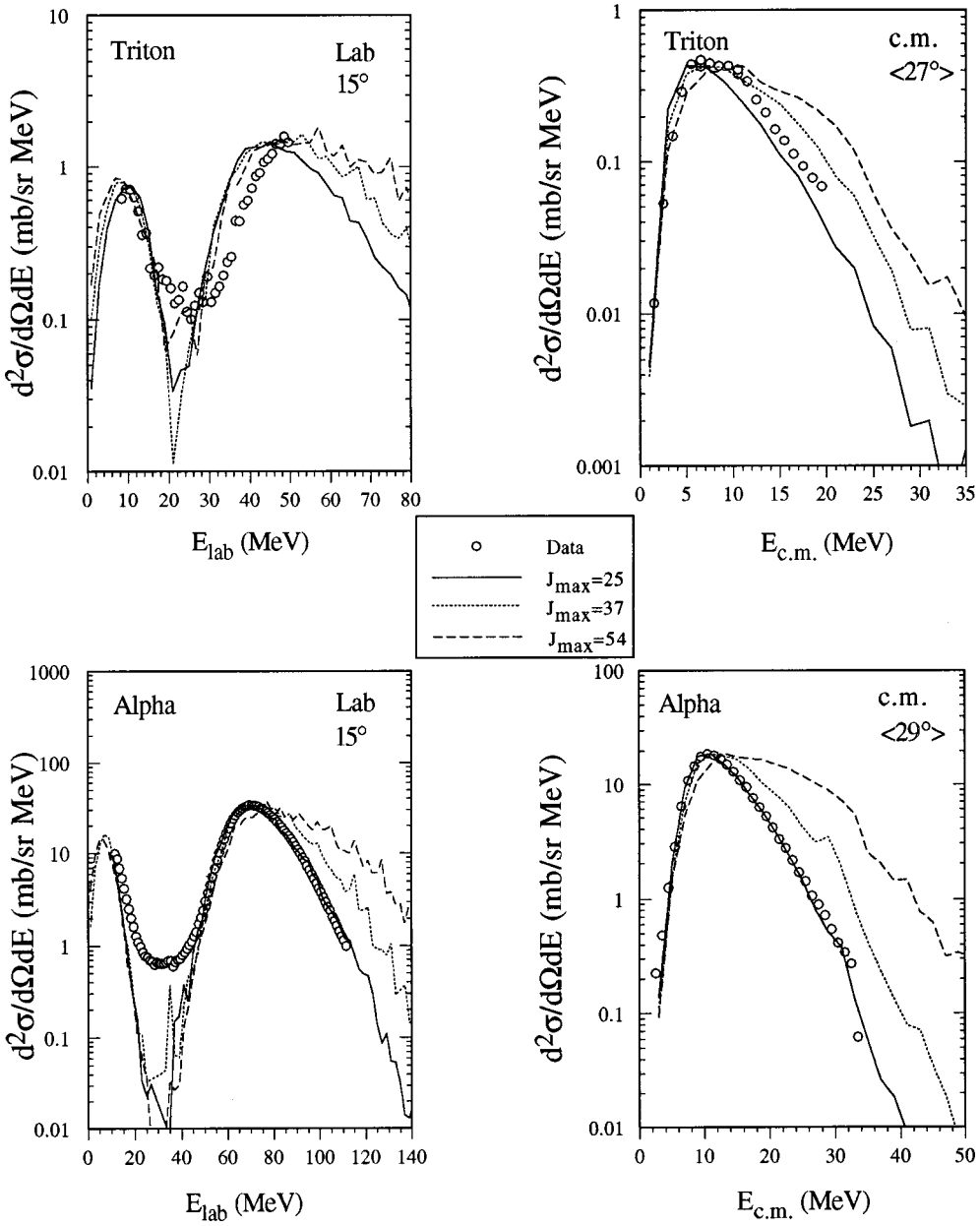

FIG. 13. Inclusive ^{3}H and ^{4}He energy spectra for the 670 MeV ^{55}Mn+^{12}C reaction, compared with MODGAN simulations using spin parameters $J_{max}=25$, 37, and 54$\hbar$. Tritons are shown in the upper panels and alphas in the lower panels, with laboratory spectra on the left and c.m. spectra on the right.

simulations, and the experimental triton c.m. spectra are approximately 2 MeV higher in energy. These observations are true for both the 280 MeV ^{40}Ar+^{27}Al and the 670 MeV ^{55}Mn+^{12}C reactions, and with either MODGAN or LILITA_N95. This systematic behavior among the evaporated $Z=1$ isotopes, namely, good fits with the proton spectra, but significantly less barrier reductions required for ^{2}H and ^{3}H, has been reported and discussed previously [1,2]. It can be understood in terms of higher nuclear-matter densities being required for the coalescence of composite particles [1].

The spin of the composite emitter I_i enters the model calculations through the Fermi gas level density [16,19–23], and through the centrifugal barrier. It always appears in the form of a ratio

$$\frac{I_i^2\hbar^2}{2\mathfrak{I}T}, \tag{1}$$

namely, the square of the spin divided by the moment of inertia $\mathfrak{I}$ and the temperature T. Therefore, while we have chosen to vary the spin (in the simulations) in order to match the experimental energy spectra, we could instead have achieved the same effect by increasing the moment of inertia (i.e., by allowing for significant deformation of the highly excited composite nuclei).

The angular distributions can be described in terms of a β_2 parameter [24,25] where the angular distribution is proportional to $\exp(\beta_2\sin^2\theta)$, and the angle θ is measured with

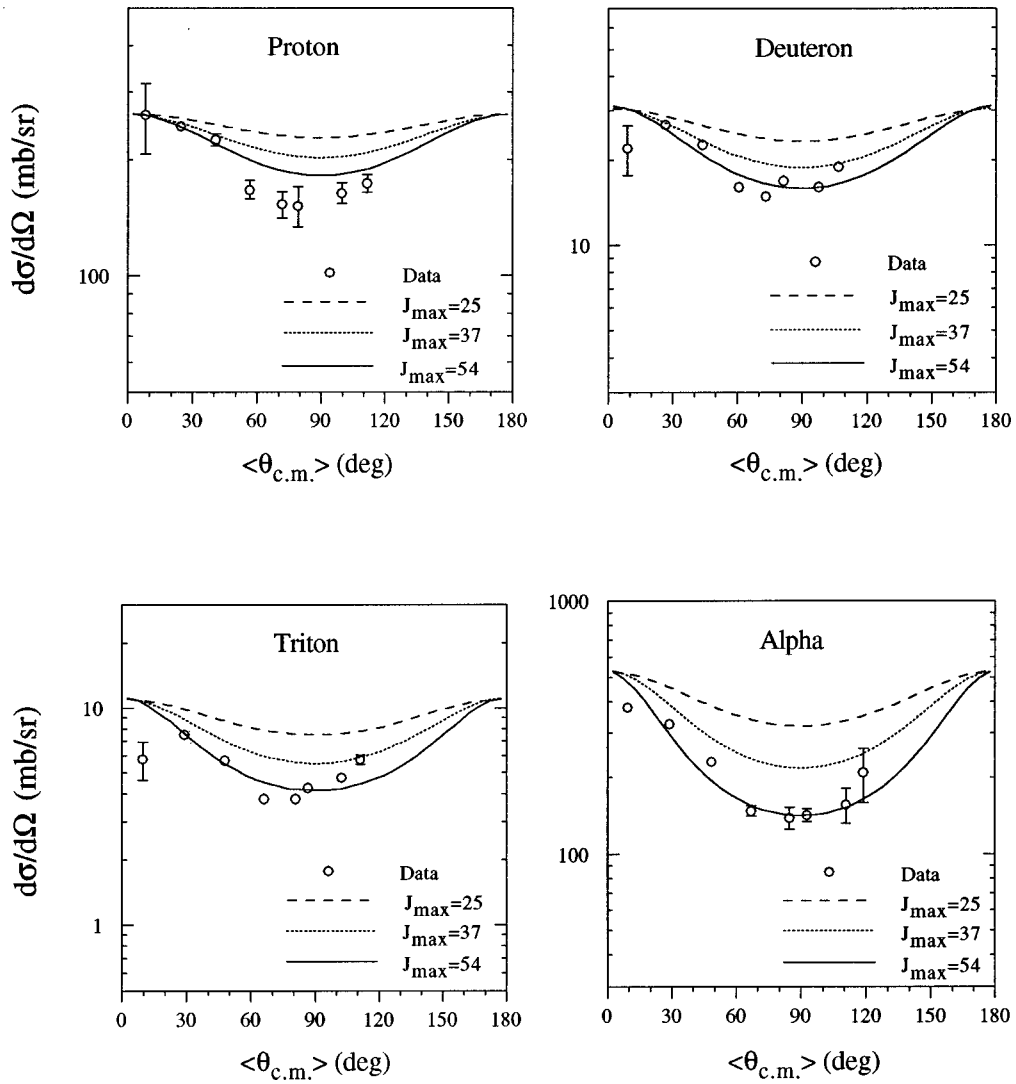

FIG. 14. Comparisons of MODGAN simulations with light particle inclusive angular distributions for the 280 MeV ^{40}Ar+^{27}Al reaction. The simulated curves are for several values of the spin parameter J_{max} as indicated.

respect to the spin direction. This parameter, β_2, has the form

$$\beta_2=\frac{\hbar^2 I_i^2}{2\Im T}\left[\frac{\mu R^2}{\Im+\mu R^2}\right], \tag{2}$$

where μ is the reduced mass of the system at the instant of particle emission. Equation (2) predicts that increasing the spin increases the anisotropy, and decreasing the temperature also increases the anisotropy. The 190 MeV ^{40}Ar+^{27}Al reaction studied by La Rana *et al.* [26] has an α singles anisotropy ratio for 15°/90° of 2.22. The 280 MeV ^{40}Ar+^{27}Al reaction has a value of 2.98 for this same quantity indicating that there is a larger anisotropy involved in the 280 MeV ^{40}Ar+^{27}Al reaction than there is in the 190 MeV ^{40}Ar +^{27}Al reaction. This is consistent with the behavior of the β_2 parameter, as the 190 MeV ^{40}Ar+^{27}Al reaction has a 20% smaller I_i^2/T ratio than does the 280 MeV ^{40}Ar+^{27}Al reaction.

The simulation codes cannot, however, predict the apparent low proton emission barriers. (This is why empirical evaporation barriers [1] were used to fit the particle spectra.) One possible explanation for this might be nuclear deformation. A nuclear distortion would increase the moment of inertia as the compound system deformed from an idealistic spherical shape, and a significantly increased moment of inertia would not be inconsistent with the observed trends in the experimental data.

There have been several studies in which the effects of nuclear deformation have been investigated [1,26,27]. In these works, the spin was fixed by using fusion cross section data and the energy spectra were then fit by allowing the nucleus to deform. It was found that with a sufficiently deformed nucleus, the α energy spectra and the proton and α angular distributions could be reproduced. However,the proton energy spectra could not be reproduced by the simulations, as no reasonable distortion would produce a large enough reduction in the proton emission barrier. Similar ob-

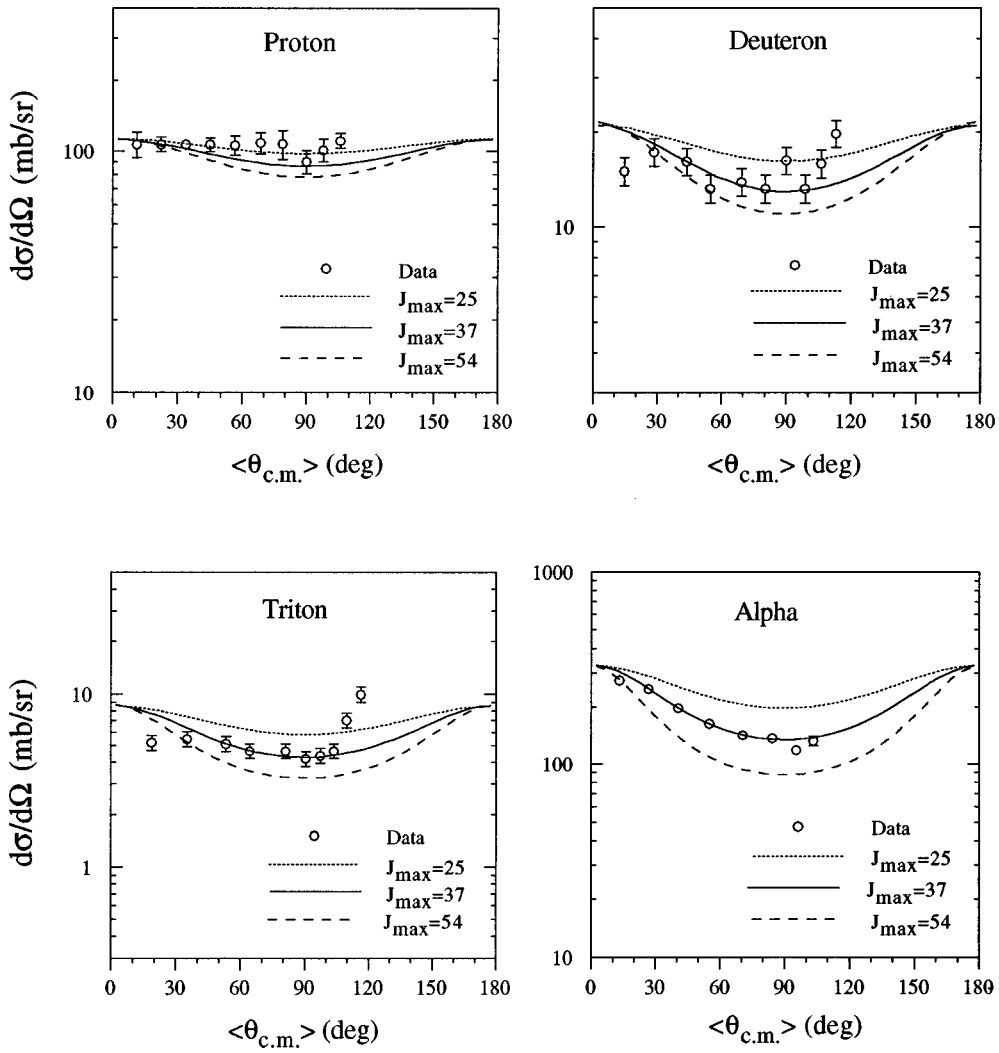

FIG. 15. Comparisons of MODGAN simulations with light particle inclusive angular distributions for the 670 MeV ^{55}Mn+^{12}C reaction. The simulated curves are for several values of the spin parameter J_{max} as indicated.

servations have been reported previously [2] for a somewhat heavier composite system ($A\sim96$) than the one being considered here.

V. CONCLUSIONS

In this investigation we have found that the statistical model is not capable of reproducing both the experimental α energy spectra and angular distributions with a single set of input parameters. Two different values of the spin J_{max} are required. A spin of $J_{max}=25\hbar\pm2\hbar$ is needed to fit the energy spectra for both the 280 MeV ^{40}Ar+^{27}Al and the 670 MeV ^{55}Mn+^{12}C reactions. A spin of $54\hbar$ is required to fit the α angular distribution from the 280 MeV ^{40}Ar+^{27}Al reaction and a spin of $37\hbar$ is needed to fit the angular distribution from the 670 MeV ^{55}Mn+^{12}C reaction. The proton energy spectra and angular distributions are not very sensitive to the spin, making it difficult to choose one spin value over another. However, the spins which fit the α energy spectra and angular distributions are consistent with the proton data as well. The ratio of particle multiplicities is also quite sensitive to emitter spin. For both reactions, the spin distributions required, in the calculational models, to reproduce the data are in agreement with the angular distribution results (and not the energy spectra).

Though the shapes of the center-of-mass α energy spectra for these two reactions are essentially the same, the respective angular distributions have substantially different anisotropies. This indicates emissions from parents with very different spin distributions, in agreement with the spin ranges derived from fusion cross section estimates.

The energy spectra of light charged particles from the 280 MeV ^{40}Ar+^{27}Al reaction, with an excitation energy of 127 MeV, have high energy slopes which are not as steep as those from the 190 MeV ^{40}Ar+^{27}Al system [26], with an excitation energy of 91 MeV. This is consistent with the predictions of the statistical model, which indicates that both higher temperatures and larger spins are involved at the higher excitation energy.

Reduced evaporation barriers [1] are required to fit the proton energy spectra. The deuterons and tritons, however, which also are $Z=1$ particles, do not seem to need as strong

a reduction as suggested by the modified charge dependence of the protons. In this charge region of emitters, the reduced barrier for α particles is very similar to its fusion barrier [1], and simulated α spectra using the fusion barriers [18] can fit the experimental data equally well.

In light of the above, particularly the inconsistency between spins derived from fitting particle angular distributions and energy spectra, care must be taken when using statistical model codes in conjunction with experimental data. The models do not seem to incorporate all of the physics required to make accurate predictions of nuclear evaporation observables, and this deficiency is most apparent for light-mass systems where spin effects are enhanced. There is enough flexibility (i.e., parameters) in the models such that apparent agreement can often be achieved with limited experimental data sets. Hence it is most important to measure multiple properties for the same system (e.g., charged particle energy spectra, angular distributions, multiplicities), in order to gain a significant test of the model.

ACKNOWLEDGMENTS

This report is based upon the Ph.D. thesis of Craig M. Brown, Carnegie Mellon University, 1997. We would like to thank the staff of the LBNL 88 Inch Cyclotron for the excellent support in carrying out these experiments. Particular appreciation goes to Bill Rathbun for assistance with the data acquisition system and for plugging holes whenever needed. N.N. Ajitanand was very helpful in the debugging and operation of the MODGAN code. This work was supported by the Division of Nuclear Physics, U.S. Department of Energy.

[1] W.E. Parker, M. Kaplan, D.J. Moses, G. La Rana, D. Logan, R. Lacey, J.M. Alexander, D.M. de Castro Rizzo, P. DeYoung, R.J. Welberry, and J.T. Boger, Phys. Rev. C **44**, 774 (1991), and references cited therein.

[2] M. Kildir, G. La Rana, R. Moro, A. Brondi, A. Dnofrio, E. Perillo, V. Roca, M. Romano, F. Terrasi, G. Nebbia, G. Viesti, and G. Prete, Phys. Rev. C **46**, 2264 (1992).

[3] F. Puhlhofer, Nucl. Phys. **A280**, 267 (1977).

[4] N.N. Ajitanand, R. Lacey, G.F. Peaslee, E. Duek, J. M. Alexander, and Nucl. Instrum. Methods Phys. Res. A **243**, 111 (1986).

[5] N.N. Ajitanand, G. La Rana, R. Lacey, David J. Moses, Louis C. Vaz, G.F. Peaslee, D.M. de Castro Rizzo, Morton Kaplan, and John M. Alexander, Phys. Rev. C **34**, 877 (1986).

[6] The code LILITA-N95 is an extensively modified version of the LILITA program originally developed by J. Gomez del Campo (Ref. [7]). It has been renamed to differentiate it from several other versions of LILITA [M. Kaplan and G. La Rana (private communication)].

[7] J. Gomez del Campo and R. G. Stokstad, Oak Ridge National Laboratory Report No. ORNL-TM-7295, 1981; J. Gomez del Campo, R.G. Stokstad, J.A. Biggerstaff, R.A. Dayras, A.H. Snell, and P.H. Stelson, Phys. Rev. C **19**, 2170 (1979).

[8] N.N. Ajitanand and J.M. Alexander, Nucl. Instrum. Methods Phys. Res. A **376**, 213 (1996).

[9] M. Kaplan, C. M. Brown, J. B. Downer, Z. Milosevich, E. Vardaci, J. P. Whitfield, C. Copi, and P. DeYoung, *Advances in Nuclear Dynamics*, edited by W. Bauer and A. Mignerey (Plenum Press, New York, 1996), p. 113.

[10] D.J. Moses, M. Kaplan, J.M. Alexander, D. Logan, M. Kildir, L.C. Vaz, N.N. Ajitanand, E. Duek, and M.S. Zisman, Z. Phys. A **320**, 229 (1985).

[11] C. M. Brown, Ph.D. Thesis, Carnegie Mellon University, 1997.

[12] R. G. Stokstad, in *Treatise on Heavy Ion Science*, edited by D. A. Bromley (Plenum Press, New York, 1985), Vol. 3, p. 83.

[13] P. Frobrich, Phys. Rep. **116**, 337 (1984).

[14] O. Civitarese and M. Schvellinger, J. Phys. G **20**, 1933 (1994).

[15] D. Bodansky, Annu. Rev. Nucl. Sci. **12**, 79 (1962).

[16] T. Ericson, Adv. Phys. **9**, 425 (1960).

[17] See, for example, H. Dumont, A. D'Onofrio, M. G. Saint-Laurent, F. Terrasi, B. Delaunay, J. Delaunay, and D. Rizzo, in Proceedings of the International Winter Meeting on Nuclear Physics, Bormio, Italy, 1980 (unpublished).

[18] L.C. Vaz and J.M. Alexander, Z. Phys. A **318**, 231 (1984).

[19] A. Bohr, and B. R. Mottelson, *Nuclear Structure* (Benjamin, New York, 1969), Vol. 1.

[20] L.M. Bollinger in *Nuclear Spectroscopy*, edited by F. Ajzenberg-Selove (Academic Press, New York, 1960), pt. A.

[21] R. M. Eisberg, *Fundamentals of Modern Physics* (Wiley, New York, 1964).

[22] A. Gilbert and A.G.W. Cameron, Can. J. Phys. **43**, 1446 (1965).

[23] E. Segre, *Nuclei and Particles*, (Benjamin, New York, 1977).

[24] T. Dossing, Licentiat thesis and unpublished notes, University of Copenhagen, Denmark, 1977.

[25] G. Catchen, M. Kaplan, J.M. Alexander, and M.F. Rivet, Phys. Rev. C **21**, 940 (1980).

[26] G. La Rana, D.J. Moses, W.E. Parker, M. Kaplan, D. Logan, R. Lacey, J.M. Alexander, and R.J. Welberry, Phys. Rev. C **35**, 373 (1987).

[27] Z. Majka, M.E. Brandan, D. Fabris, K. Hagel, A. Menchaca-Rocha, J.B. Natowitz, G. Nebbia, G. Prete, B. Sterling, and G. Viesti, Phys. Rev. C **35**, 2125 (1987).